Streambed scour and fill in low-order dryland channels

D. Mark Powell

Department of Geography, University of Leicester, Leicester, UK

Richard Brazier and John Wainwright

Department of Geography, University of Sheffield, Sheffield, UK

Anthony Parsons and Jörg Kaduk

Department of Geography, University of Leicester, Leicester, UK

[1] Distributions of scour and fill depths recorded in three low-order sand bed dryland rivers were compared with the Weibull, gamma, exponential, and lognormal probability density functions to determine which model best describes the reach-scale variability in scour and fill. Goodness of fit tests confirm that the majority of scour distributions conform to the one-parameter exponential model at the 95% significance level. The positive relationship between exponential model parameters and flow strength provides a means to estimate streambed scour depths, at least to a first approximation, in comparable streams. In contrast, the majority of the fill distributions do not conform to the exponential model even though depths of scour and fill are broadly similar. The disparities between the distributions of scour and fill raise questions about notions of channel equilibrium and about the role of scour and fill in effecting channel change.

Citation: Powell, D. M., R. Brazier, J. Wainwright, A. Parsons, and J. Kaduk (2005), Streambed scour and fill in low-order dryland channels, *Water Resour. Res.*, *41*, W05019, doi:10.1029/2004WR003662.

1. Introduction

[2] Soundings made from bridge crossings and at gauging station cable crossings commonly reveal fluctuations in the vertical position of an alluvial streambed during flood events [e.g., *Leopold and Maddock*, 1953]. The fluctuations occur in response to the entrainment (or scour) and deposition (or fill) of bed material and reflect both the redistribution of sediment within the channel and the short-term hydraulic adjustments that help a river to maintain a quasi-equilibrium channel form [*Andrews*, 1979]. As a result, scour and fill processes have been of longstanding interest to geomorphologists, engineers and aquatic ecologists seeking to understand the morphodynamics of alluvial rivers [*Haschenburger*, 1999], the stability of artificial structures such as bridge piers, pipelines and water abstraction points [*Chang*, 1988] and the role of flood disturbance in structuring lotic ecosystems [*Lapointe et al.*, 2000; *Rennie and Millar*, 2000].

[3] Although scour and fill are characteristic of all alluvial rivers, they are of particular importance in dryland environments where there is effectively an unlimited supply of sandy-gravelly material that is readily entrained by infrequent, but intense, flooding [*Leopold et al.*, 1966]. Some studies have suggested that scour tends to occur in reaches that are narrow and deep, whereas wide and shallow reaches tend to aggrade [*Lane and Borland*, 1954]. This dynamic is thought to reflect the control of channel width on unit discharge and as a result, a predictive relationship between unit discharge and scour depths has been identified

[*Leopold et al.*, 1966]. Other studies have shown depth and continuity of scour to be independent of cross-sectional morphology [*Emmett and Leopold*, 1965] and to be consistent with the migration of bed forms [*Foley*, 1971].

[4] This uncertainty over channel bed behavior during flood flows arises because few studies have featured measurements of sufficient density to characterize the magnitude and distribution of scour and fill occurring within a reach. Gauging station measurements are limited because they are restricted to observations made at isolated cross sections while other studies [e.g., *Leopold et al.*, 1966] are constrained by the low density of data acquisition. As a result, it is not known whether scour and fill are localized phenomena or are more or less continuous along the stream. Some progress has been made in characterizing the reach-scale variability of scour and fill in coarse-grained perennial rivers. *Haschenburger* [1999], for example, has shown that scour depth populations in gravel bed rivers are characterized by negative exponential populations, and *Rennie and Millar* [2000] have shown that spatial patterns of scour in the coarse-grained Kanaka Creek, British Columbia, Canada, are essentially random. Very little, however, is known about reach-scale variability of scour and fill in sand bed rivers, even though it is known that such rivers are particularly susceptible to scour and fill, and that the associated convergence and divergence in sediment transport rates control their morphological development.

[5] The aim of this paper is to present a statistical analysis of event-based measurements of scour and fill made in three reaches of low-order sand bed rivers. The objective is to determine the best distributional model to describe the reach-scale variability in scour and fill depths recorded over
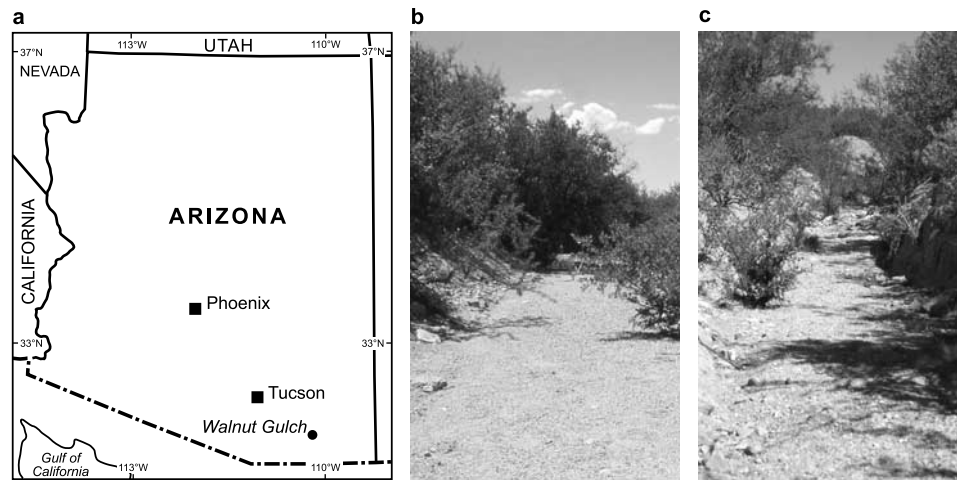
Figure 1. (a) Location of study area at Walnut Gulch, SE Arizona and views of (b) the main channel reach and (c) the upper tributary reach.

a range of competent flows. Four plausible model distributions are tested to answer three basic questions (http://www.itl.nist.gov/div898/handbook/): (1) Does a given distributional model provide an adequate fit to the data? (2) Of the candidate distributional models, is there one distribution that fits the data better than the other candidate distributional models? (3) Can the findings be generalized to provide a simple model for predicting scour and fill depths in sand bed streams.

2. Field Site

[6] The study was conducted within the Walnut Gulch Experimental Watershed of the United States Department of Agriculture, Agricultural Research Service, in southeastern Arizona (Figure 1a). Walnut Gulch is a sand- and gravel-bedded, ephemeral stream channel draining a dissected grass- and shrub-covered piedmont composed primarily of weakly consolidated Quaternary alluvium [*Lane et al.*, 1997]. The climate is semiarid with a mean annual rainfall of 350 mm. Virtually all of the runoff occurs during the summer months, and results from intense, short-lived and highly localized convective storms [*Renard and Keppel*, 1966; *Renard and Laursen*, 1975].

[7] Measurement efforts were concentrated in three reaches within Lucky Hills, a 0.47 km² subcatchment of the main watershed [*Nichols*, 1999]. One reach was located on the main channel (MCR) (Figure 1b) and two reaches were located in upper and lower tributary channels (UTR and LTR, respectively) (Figure 1c). All three reaches were straight, single thread and relatively narrow and steep. The beds were planar and composed of a poorly sorted and spatially undifferentiated mixture of sand and fine

gravel (Table 1). Although typical of headwater streams within the Walnut Gulch drainage network, these sedimentological characteristics are not representative of the higher-order stream channels, many of which exhibit low relief, gravel bar forms and short reaches of predominantly gravel-sized bed material.

3. Methods

[8] Scour and fill data were collected by means of scour chains [*Emmett and Leopold*, 1965; *Laronne et al.*, 1994]. Scour chains provide information on maximum depths of scour and net depths of fill and therefore offer advantages over conventional survey techniques that only provide estimates of net channel change (scour or fill). Scour chains, however, cannot provide data pertaining to the temporal variation in scour and fill and to bed elevation changes associated with multiple cycles of scour and fill during a single event. Such information can only be gathered with more sophisticated electronic scour monitors [e.g., *De Vries et al.*, 2001]. However, such sophistication entails great expense and thus would be impracticable for investigating the distributions of scour and fill, which is the central aim of the paper.

[9] In each of the three study reaches, scour chains were inserted across 30 cross sections located one channel width apart for a downstream distance of 30 channel widths. In the absence of any a priori information about the variability of scour and fill in sand bed channels, this pattern was considered sufficient to characterize the reach-scale variability in depths of scour and fill. Three to five chains were installed at equally spaced distances across each cross section in the relatively wide main channel and lower

Table 1. Characteristics of the Study Reaches

Site	Reach Length, m	Number of Chains	Width,[a] m	Depth,[b] m	Discharge, m³ s⁻¹	Slope, %	D_{50}, mm
MCR	87.0	99	3.1	0.45	0.21–11.4	1.9	1.3
UTR	29.8	45	1.2	0.75	0.03–1.05	1.9	2.2
LTR	58.7	95	2.0	0.42	0.04–1.23	1.7	1.2

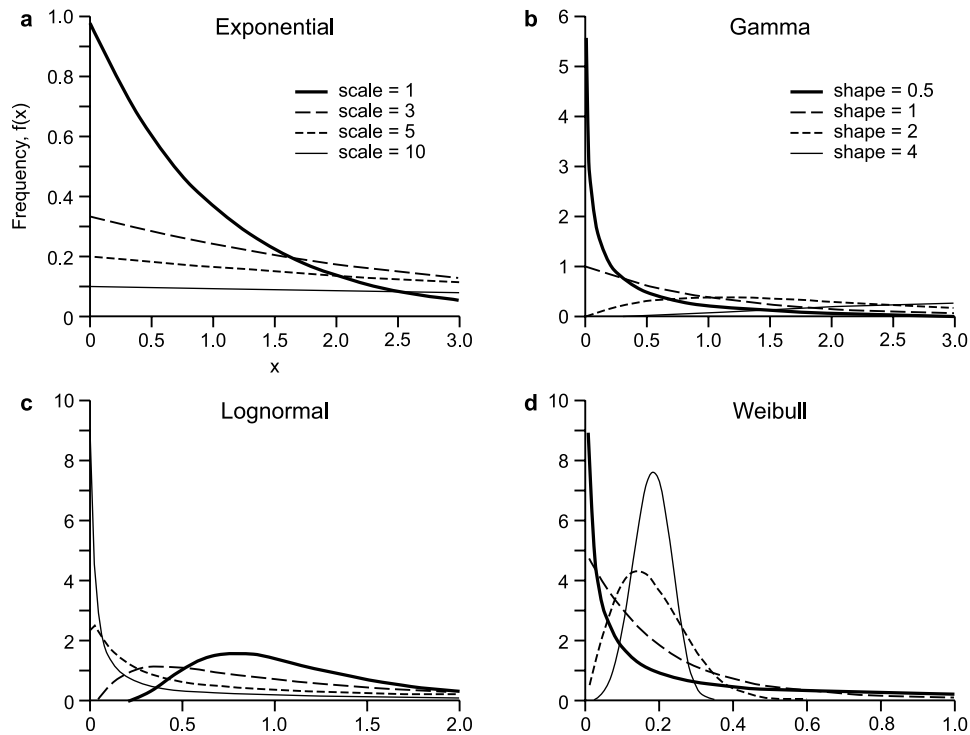[a]Mean bed width for reach.
[b]Bank-full depth.

Figure 2. Shapes of (a) exponential, (b) gamma, (c) lognormal, and (d) Weibull frequency distributions. The exponential distribution is monotonic and always concave; the shape of the gamma, lognormal, and Weibull distributions can take a variety of forms depending on the value of the shape parameter (γ). For all distributions the scale parameter (α) has the effect of stretching the distribution as it increases in value, as illustrated for the exponential distribution (Figure 2a).

tributary reaches. In the narrower upper tributary reach, chains were installed in an alternating sequence of one in the channel center and two at left and right locations. This pattern ensured that adjacent chains did not become entangled. Accordingly, the number of chains installed in each reach ranged from 45 in the upper tributary reach to 99 in the main channel reach (Table 1). Chain densities varied between 0.36 and 1.3 m^{-2}, values that exceed those in previous studies by two to three orders of magnitude [*Rennie and Millar*, 2000]. Scour chain recovery after each competent flood event always exceeded 97% of the total installed at each site.

[10] Flows in the main channel were measured with an ultrasonic depth recorder that was logged at 30-s intervals. Flows in the tributaries were monitored with maximum stage recorders and as a result, hydraulic information is restricted to peak flow depths (Y_p). At all locations, estimates of flow depth were converted to discharge (Q) using Manning's equation. Estimates of channel average shear stress (τ, N m^{-2}) were derived as $\tau = \rho gRS$ in which ρ is the density of the flow (kg m^{-3}), g is the acceleration due to gravity (m s^{-2}), R is the hydraulic radius (m) and S is the surveyed bed slope (m m^{-1}).

4. Probability Distribution Functions

4.1. Selection of Suitable Probability Distribution Functions for Modeling Scour and Fill in Sand Bed Streams

[11] Reach-scale distributions of scour and fill depths in perennial gravel bed rivers have been modeled using the exponential probability density function (pdf) [*Haschenburger*, 1999]. The exponential pdf is defined by

$$p(x) = \frac{1}{\alpha} \exp\left(-\frac{x - \lambda}{\alpha}\right), x > \lambda; \alpha > 0 \qquad (1)$$

in which p(x) is the probability of scour (or fill) occurring to a depth of x cm, and α and λ are the scale and location parameters, respectively. The location parameter locates the distribution along the abscissa and has the same units as the variable being modeled (i.e., cm). If $\lambda = 0$, then the distribution starts at the origin (x = 0). Positive and negative location parameters shift the distribution λ units to the right and left, respectively. The scale parameter stretches or compresses the distribution. Because the exponential pdf starts at x = λ at the level p(x = λ) = $1/\alpha$ and decreases exponentially thereafter (i.e., p(x) → 0 as x → 8), the shape of the distribution is always monotonic and concave up (Figure 2a).

[12] *Haschenburger* [1999] employed the one-parameter exponential pdf in which $\lambda = 0$ to characterize the reach-scale variability of scour and fill in gravel bed streams. The choice of the one-parameter exponential model reflects the widespread view that bed material movement in coarse-grained rivers is a close-to-threshold process and that although limited areas may scour or fill relatively deeply, most gravel beds experience little, if any, activity during competent flow events. Such a dynamic, however, may not be observed in steep sand bed rivers where high excess shear stresses and mobile bed sediments may cause much of the sand bed to scour (and subsequently fill) at quite modest
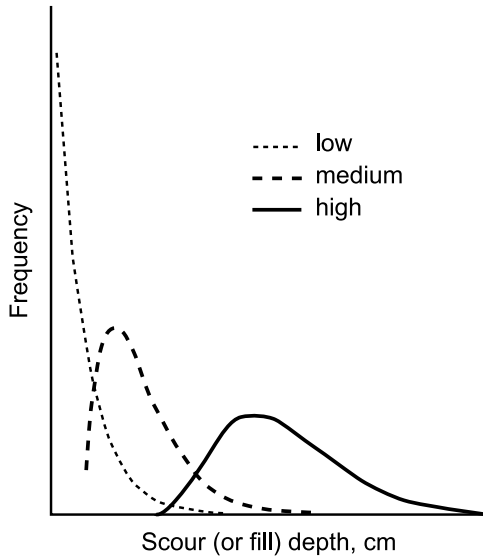
Figure 3. Hypothesized frequency distributions of scour (or fill) depths in a sand bed stream at low, medium, and high discharges. At all but the lowest competent flows the whole of the channel bed is activated (scoured or filled), and the depths of scour (or fill) increase with flow magnitude. As a result, both the location and shape of the distribution change with increasing flow strength.

flows and depths of scour (and subsequent fill) to increase dramatically with flow strength. As a result, more flexible models in which both the location and shape of the distributions can vary with flow strength may be required to describe the distributions of scour and fill in sand bed streams [*Hassan et al.*, 1999] (Figure 3).

[13] Additional flexibility is provided by distributions that incorporate a third parameter (γ) that allows them to take on a variety of shapes depending on its value. The

gamma, lognormal, and Weibull probability density functions incorporate shape parameters and have variously been used to model a wide range of geomorphological variables including particle travel distances and burial depths [*Hassan et al.*, 1991, 1999], bed form amplitude [*Paola and Borgman*, 1991], and wind speed and particle size distributions [*Takle and Brown*, 1978; *Zobeck et al.*, 1999; *Kondolf and Adhikari*, 2000]. These three-parameter pdfs are defined by equations (2)–(4):

Gamma

$$p(x) = \frac{(x-\lambda)^{\gamma-1}}{\alpha^{\gamma}\Gamma(\gamma)} \exp\left(-\frac{x-\lambda}{\alpha}\right), x > \lambda; \alpha, \gamma > 0 \quad (2)$$

in which Γ is the gamma function;

Lognormal

$$p(x) = \frac{1}{\gamma(x-\lambda)\sqrt{2\pi}} \exp\left(-\frac{(\ln((x-\lambda)/\alpha))^2}{2\gamma^2}\right), x > \lambda; \alpha, \gamma > 0; \quad (3)$$

Weibull

$$p(x) = \frac{\gamma}{\alpha}\left(\frac{x-\lambda}{\alpha}\right)^{\gamma-1} \exp\left(-\left(\frac{x-\lambda}{\alpha}\right)^{\gamma}\right), x > \lambda; \alpha, \gamma > 0. \quad (4)$$

The effect of different values of the shape parameter on the shape of gamma, lognormal, and Weibull frequency distributions is shown in Figures 2b–2d and summarized in Table 2. The ability to model a range of distributional shapes with a single distributional model makes each of these distributions more flexible than the exponential distribution which only has one shape. They may potentially

Table 2. Characteristic Shapes of the Lognormal, Weibull, and Gamma pdfs for Different Values of the Shape Parameter[a]

Distribution	Shape Parameter	Shape of Probability Density Function
Lognormal	$\gamma > 0$	The pdf is positively skewed (has a right tail); starts at zero, increases to mode and decreases thereafter. If $\gamma \gg 1$ then the pdf rises very sharply for small values of x and essentially follows the ordinate axis, peaks out early and then decreases sharply like an exponential pdf or a Weibull pdf with $0 \leq \gamma \leq 1$.
Weibull	$0 \leq \gamma < 1$	As $x \to 0$ (or λ), $p(x) \to \infty$; as $x \to \infty$, $p(x) \to 0$, i.e., $p(x)$ decreases monotonically and is concave as x increases beyond the value of α and the mode is nonexistent.
Weibull	$\gamma = 1$	The pdf is the two-parameter exponential distribution.
Weibull	$\gamma > 1$	$p(x) = 0$ at $x = 0$ (or λ); $p(x)$ increases as $x \to x'$ (the mode) and decreases thereafter.
Weibull	$\gamma < 2.6$	The pdf is positively skewed (has a right tail).
Weibull	$2.6 \leq \gamma \leq 3.7$	The skewness of the pdf approaches zero (no tail).
Weibull	$\gamma > 3.7$	The pdf is negatively skewed (has a left tail).
Gamma	$0 \leq \gamma < 1$	As $x \to 0$ (or λ), $p(x) \to \infty$; as $x \to \infty$, $p(x) \to 0$, i.e., $p(x)$ decreases monotonically and is concave as x increases beyond the value of α and the mode is nonexistent.
Gamma	$\gamma = 1$	The pdf is the two-parameter exponential distribution
Gamma	$\gamma > 1$	The pdf is positively skewed (has a right tail); starts at zero, increases to mode and decreases thereafter.

[a]The case where $\lambda = 0$ defines the two-parameter version of the pdf in each case. Note that the gamma and Weibull distributions converge to the exponential distribution as $\lambda \to 1$ and conform to the exponential distribution when $\lambda = 1$ (see equations (2) and (4)).

Table 3. Initial Values of the Parameters α, γ, and λ (α_0, γ_0, and λ_0) Utilized in the Maximum Likelihood Procedure[a]

	λ_0	α_0	γ_0	Variable Definition
Exponential	0	m	-	$m = \frac{\sum_{i=1}^{N} x_i}{N}$
Gamma	0	m	1	$m = \frac{\sum_{i=1}^{N} x_i}{N}$
Lognormal	0	$\exp(\bar{\mu})$	$\sqrt{\frac{\sum_{i=1}^{N} (\ln(x_i - \bar{\mu}))^2}{N}}$	$\bar{\mu} = \frac{\sum_{i=1}^{N} \ln(x_i)}{N}$
Weibull	0	$\hat{X}/\ln(2)$	1	$\hat{X}$ = sample median

[a]N is the number of observations in the distribution.

therefore be better candidates for modeling the reach-scale variability of scour and fill in sand bed streams.

4.2. Parameter Estimation

[14] The parameters of a probability distribution can be estimated using a variety of methods. In this study, the parameters of the distributions were estimated using maximum likelihood methods using Matlab programs [*The MathWorks*, 2000]. The direct search algorithm employed in the maximization procedure is based on a simplex search method as implemented by the Matlab function "fminsearch." Confidence intervals (95%) for shape and scale parameters were calculated using the Matlab functions "expfit," "gamfit" and "weibfit" [*The MathWorks*, 2000]. It should be noted that the location parameter often drifted below zero during the numerical optimization. Since a negative location parameter has no physical meaning in the context of a depth distribution, λ was constrained to be ≥ 0. The results therefore are maximum likelihood parameters for which $\lambda \geq 0$.

[15] The numerical optimization procedure requires initial values α_0, λ_0 and γ_0 for the parameters α, λ, and γ respectively (Table 3). Since $\lambda \geq 0$, and λ is expected to be small, $\lambda_0 = 0$. α_0 for the exponential and the lognormal distributions and γ_0 for the lognormal distributions were calculated as the MLEs of α and γ respectively [*Johnson et al.*, 1994, pp. 207, 220, 223, 506]. For the gamma and Weibull distributions, α_0 was estimated as the MLE of α after the simplifying assumption that $\gamma_0 = 1$ was made [*Johnson et al.*, 1994, pp. 361, 660].

4.3. Goodness of Fit

[16] The similarity between the empirical and theoretical distributions was evaluated using root mean square error (RMSE) statistics and probability plots [*Filliben*, 1975]. RMSE statistics provide a measure of the absolute error between the observed and theoretical distributions and were calculated for each candidate distribution as

$$ RMSE = \sqrt{\frac{\sum_{i=1}^{n} \left(x_{o_i} - x_{p_i} \right)^2}{n}} \tag{5} $$

in which x_o and x_p are observed and predicted frequencies of depths falling within specified bin classes and n is the number of bin classes. RMSE statistics provide a quantitative estimate of the difference between the observed and fitted distributions. Probability plots and associated probability plot correlation coefficients (PPCCs) for each

candidate distribution were calculated using the software package 'DATAPLOT' (http://www.itl.nist.gov/div898/software/dataplot/homepage.htm). Although probability plots are used primarily as a graphical technique for determining scale and location parameters of theoretical distributions [*Chambers et al.*, 1983], they can also be used to assess how well a particular distribution resembles an observed distribution when the parameters of the former have been estimated using other techniques (e.g., maximum likelihood methods). There are two stages to the interpretation of the probability plots in terms of goodness of fit comparisons [*Chambers et al.*, 1983, p. 199]. First, the linearity of the probability plot as quantified by the PPCC is used to judge whether the data and reference distribution have the same distributional shape. Second, the probability plot is compared to the line $Y = \lambda + \alpha X$ to evaluate the acceptability of the location and scale parameter estimates. Good distributional fits are characterized by near-linear probability plots (with high PPCCs) that conform to the line $Y = \lambda + \alpha X$: nonlinear probability plots (with low PPCCs) indicate that the shapes of the distributions do not match, whereas shifts and tilts away from the line $Y = \lambda + \alpha X$ indicate differences in location and spread respectively. Mean values of RMSEs and PPCCs are denoted by $\overline{RMSE}$ and $\overline{PPCC}$, respectively.

5. Results

5.1. Characteristics of Flow Events

[17] Ten flow events were monitored during a 3 year study period. The bed of the main channel reach was activated in all 10 events. Most of the flows were single peak discharge events and included one overbank flow ($Q_p = 11.4 \text{ m}^3 \text{ s}^{-1}$) and two bank-full flows, ($Q_p \approx 4 \text{ m}^3 \text{ s}^{-1}$). The hydrograph time of rise for the six largest events ranged from 3 to 44 min with average rates of rise of up to 0.09 m per min. In keeping with expectations of flash flood behavior, flow durations were short at between 40 and 120 min. In the tributaries, nine of the 10 flow events activated the bed. As expected, peak discharges estimated from the maximum stage recorders were substantially lower than those recorded in the main channel; the highest flows of about 1 $\text{m}^3 \text{ s}^{-1}$ were about 0.1 of the highest flow in the main channel reach.

5.2. Distributions of Scour and Fill Depths

[18] The distributions of scour and fill depths for the 10 events recorded in the main channel reach are shown in Figure 4 together with the frequency distributions of the fitted exponential, gamma, lognormal, and Weibull pdfs. The data are grouped into 2 cm class intervals. Both sets of distributions are ranked from smallest to largest according to peak discharge (Q_p) to show how the range and shape of the depth distributions vary with discharge. Maximum likelihood parameter estimates for the theoretical distributions and values of the root mean square error (RMSE) statistics and probability plot correlation coefficients (PPCCs) are shown in Table 4 together with values of peak discharge and shear stress (τ_p).

[19] Median scour depths ranged from 1.1 to 15.6 cm with higher flows generating greater depths of scour over an increasing proportion of the bed. For example, during the two lowest flows ($Q_p \approx 0.3 \text{ m}^3 \text{ s}^{-1}$) about two thirds of the
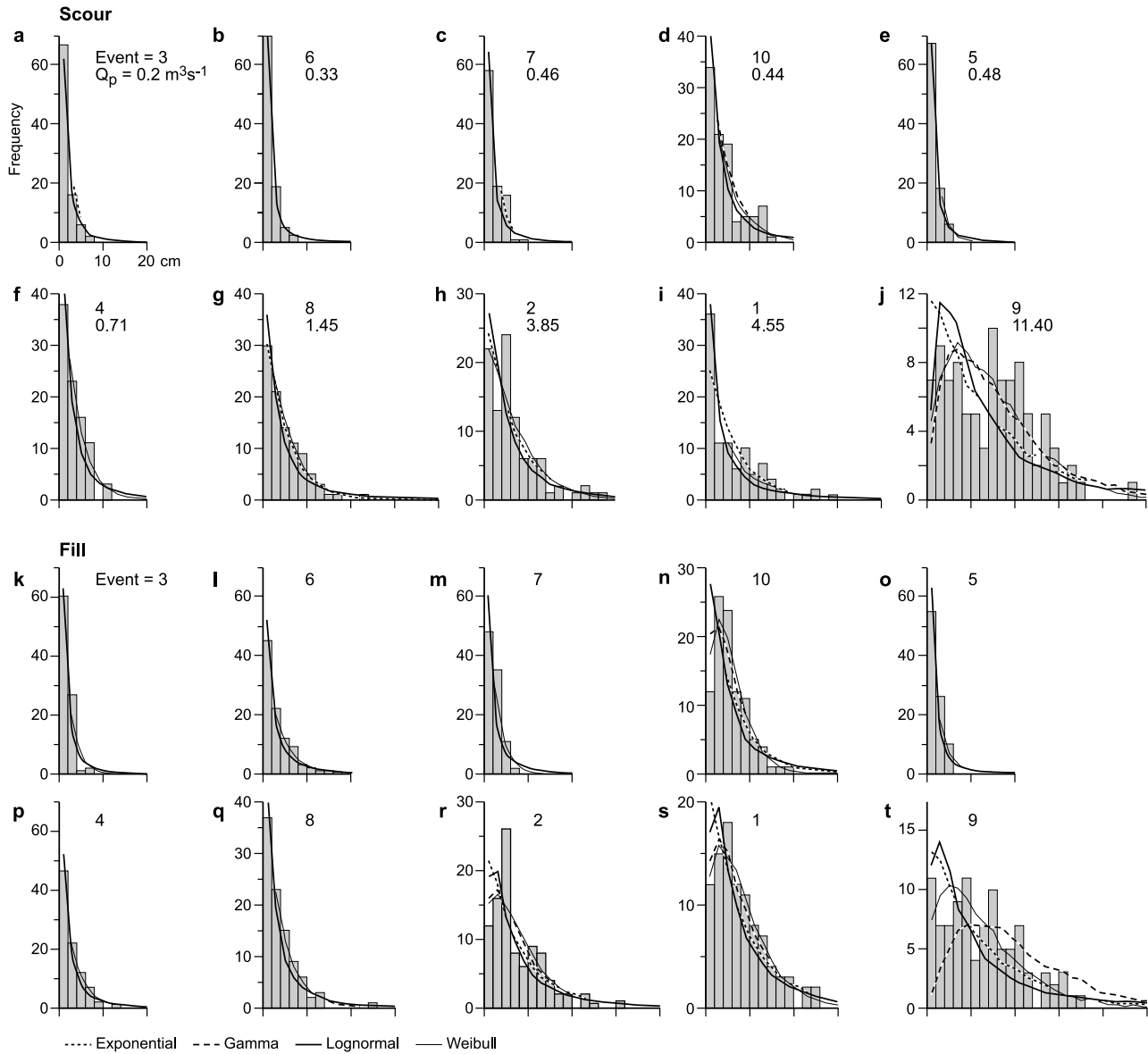
Figure 4. Frequency distributions of depths of (a–j) scour and (k–t) fill for the 10 events recorded in the main channel. Note that events 1 and 2 are bank-full events and event 9 is an overbank event.

bed experienced scour of less than 2 cm and elsewhere, bed activity did not exceed 10 cm (Figures 4a and 4b). In contrast, the highest discharge (Q_p = 11.4 m^3 s^{-1}) activated all areas of the bed and generated significant scour (>15 cm) over 50% of the bed with maximum scour depths approaching 50 cm (Figure 4j). Significant areas of the bed remained relatively stable at high discharges. During the two bank-full events, for example, up to 25% of the bed area experienced scour of less than 2 cm (Figures 4h–4i). Median depths of fill ranged from 1-12 cm (Figures 4k–4t) with a maximum of 53 cm occurring during the largest event (Figure 4t). Mean differences between paired depths of scour and fill for individual events were small, ranging from 1.1 to 4.1 cm with standard errors of 1 and 2.5 cm, respectively. Paired values of scour and fill depths differed, on average, by only 1.7 ± 2.0 cm for small flows (Q_p < 0.5 m^3 s^{-1}) and by 2.7 ± 2.4 cm for the larger flows. The Mann-Whitney test statistic indicates that only in events 1, 6 and 10 were there

significant differences between the scour and fill distributions (p < 0.05). In these events, median depths of fill exceeded median depths of scour by 2.5, 1.4 and 1.6 cm, respectively.

[20] The distributions of scour depths for the nine within-bank flow events are all monotonic and concave (Figures 4a–4i) and are well described by the exponential model (RMSEs = 1.07 to 4.69 cm; PPCCs = 0.941 to 0.997). The Weibull and gamma distributions also perform well with similar RMSEs and PPCCs (Table 4). Comparison of the exponential, Weibull, and gamma probability plots confirm that the three distributional models provide good descriptions of the scour depth distributions measured during within-bank flow events (Figure 5). The similarity in descriptive performance is not surprising given that all but one of the Weibull and gamma models fitted to data collected from subbank-full flows have shape parameters that do not differ significantly from one (p < 0.05; Table 4). As noted in Table 3, Weibull and gamma distributions with

Table 4. Exponential, Lognormal, Gamma, and Weibull Parameter Estimates and RMSE and PPCC Statistics for Distributions of Scour and Fill Depths in the Main Channel Reach[a]

Event	Q_p, m³ s⁻¹	τ_p, N m⁻²	Exponential				Lognormal					Gamma					Weibull				
			α	λ	RMSE	PPCC	γ	α	λ	RMSE	PPCC	γ	α	λ	RMSE	PPCC	γ	α	λ	RMSE	PPCC
Scour																					
3	0.21	14.6	1.85	0.02	4.43	0.995	1.25	1.11	0	2.37	0.927	1.07	1.76	0	4.22	0.996	0.99	1.84	0.02	4.38	0.995
6	0.33	17.4	1.57	0.02	1.07	0.997	1.32	0.85	0	4.65	0.920	0.92	1.72	0	2.31	0.997	0.88	1.48	0.01	2.55	0.994
7	0.46	20.1	2.09	0.02	4.69	0.983	1.46	1.01	0	8.18	0.912	0.81	2.60	0	5.93	0.983	0.85	1.94	0.01	5.97	0.982
10	0.46	20.1	4.46	0.03	3.35	0.978	1.34	2.52	0	6.18	0.925	0.99	4.56	0	4.16	0.978	0.92	4.30	0.04	3.81	0.977
5	0.48	21.5	1.59	0.01	1.38	0.941	1.32	0.88	0	4.44	0.985	0.93	1.73	0	1.64	0.943	0.87	1.50	0.02	1.75	0.955
4	0.71	25.3	3.35	0.04	3.97	0.990	1.30	1.99	0	6.31	0.925	1.08	3.14	0	4.63	0.990	1.04	3.41	0.02	3.93	0.990
8	1.45	35.0	5.01	0.04	1.46	0.989	1.26	3.05	0	3.10	0.950	1.11	4.56	0	1.99	0.989	1.06	5.12	0.04	1.44	0.989
2	3.85	53.7	6.63	0.06	3.36	0.994	1.24	4.11	0	4.36	0.927	1.16	5.77	0	3.29	0.994	1.10	6.88	0.03	3.18	0.994
1	4.55	56.8	6.57	0.03	3.93	0.992	1.58	3.07	0	2.68	0.831	0.78[b]	8.48	0	2.08	0.987	0.79[b]	5.89	0.03	2.43	0.974
9[c]	11.4	83.1	14.72	0.16	2.52	0.963	1.02	10.60	0	2.58	0.900	1.76[b]	9.08	0	2.11	0.982	1.45[b]	16.28	0.00	2.06	0.989
Minimum			1.57	0.01	1.07	0.941	1.02	0.85	0	2.37	0.831	0.78	1.72	0	1.64	0.943	0.79	1.48	0.00	1.44	0.955
Maximum			14.72	0.16	4.69	0.997	1.58	10.60	0	8.18	0.985	1.76	9.08	0	5.93	0.997	1.45	16.28	0.04	5.97	0.995
Mean					3.02	0.982				4.49	0.920				3.24	0.984				3.15	0.984
Fill																					
3	0.21	14.6	1.76	0.02	4.67	0.977	1.36	0.97	0	7.21	0.849	0.96	1.86	0	5.24	0.975	0.89	1.68	0.02	5.22	0.966
6	0.33	17.4	3.46	0.02	1.82	0.997	1.48	1.72	0	3.36	0.890	0.84	4.18	0	1.27	0.996	0.82[b]	3.16	0.02	1.22	0.990
7	0.46	20.1	2.20	0.02	8.43	0.967	1.31	1.30	0	11.89	0.895	1.07	2.10	0	9.20	0.968	1.05	2.23	0.02	7.68	0.969
10[d]	0.46	20.1	5.65	0.04	6.58	0.968	1.19	3.87	0	7.06	0.948	1.46[b]	3.92	0	3.83	0.968	1.39[b]	6.16	0.00	2.66	0.956
5	0.48	21.5	1.88	0.02	6.33	0.970	1.37	1.03	0	10.48	0.809	0.95	2.02	0	7.09	0.997	0.88	1.78	0.02	6.83	0.954
4	0.71	25.3	2.94	0.02	1.69	0.998	1.42	1.52	0	3.62	0.898	0.87	3.43	0	1.71	0.983	0.83[b]	2.71	0.02	1.83	0.991
8	1.45	35.0	4.13	0.04	1.80	0.983	1.33	2.34	0	3.87	0.946	1.01	4.15	0	2.69	0.994	0.92	3.98	0.03	2.33	0.985
2[d]	3.85	53.7	7.77	0.06	4.12	0.990	1.14	5.20	0	4.12	0.924	1.36[b]	5.79	0	3.42	0.992	1.25	8.35	0.01	3.34	0.995
1[d]	4.55	56.8	8.24	0.06	2.96	0.984	1.12	5.65	0	3.08	0.902	1.42[b]	5.88	0	1.53	0.993	1.32[b]	8.95	0.00	1.13	0.996
9	11.4	83.1	12.81	0.09	2.60	0.977	1.23	8.47	0	3.12	0.886	2.28	8.84	0	2.15	0.968	1.32[b]	13.84	0.00	2.07	0.992
Minimum			1.76	0.02	1.69	0.967	1.12	0.97	0	3.08	0.809	0.84	1.86	0	1.27	0.968	0.82	1.68	0.00	1.13	0.954
Maximum			12.81	0.09	8.43	0.998	1.48	8.47	0	11.89	0.948	2.28	8.84	0	9.20	0.997	1.39	13.84	0.03	7.68	0.996
Mean					4.10	0.981				5.78	0.895				3.81	0.983				3.43	0.979

[a]All distributions are concave and monotonic except where indicated. Other notation is explained in the text.
[b]Shape parameters significantly different from 1 (p < 0.05).
[c]Distributions are bimodal.
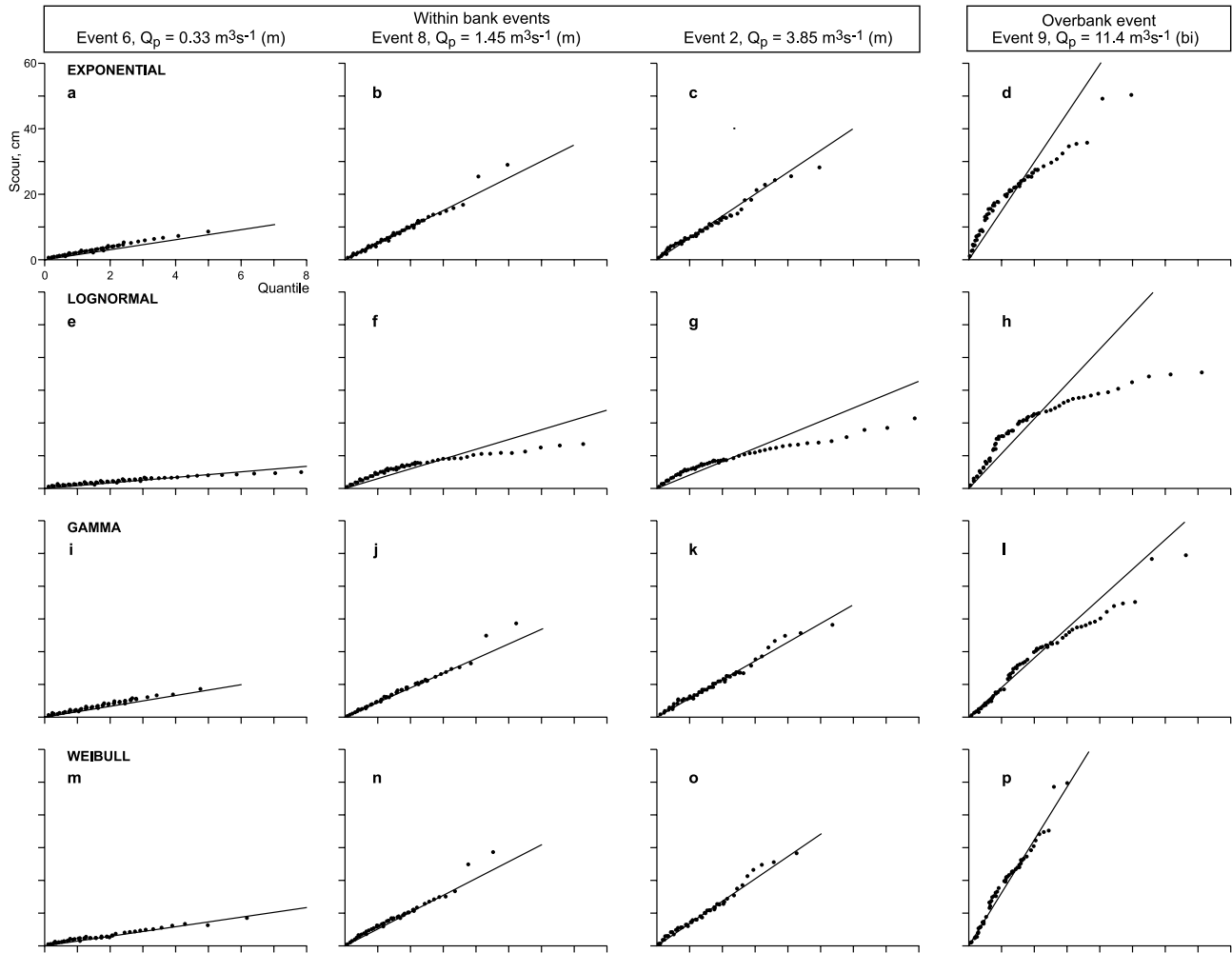[d]Distributions are skew-peaked.

Figure 5. Probability plots for the theoretical pdfs fitted to monotonic (m) scour distributions obtained at discharges representative of low ($Q_p = 0.33$ m^3 s^{-1}), medium ($Q_p = 1.45$ m^3 s^{-1}), and high ($Q_p = 3.85$ m^3 s^{-1}) within-bank flow events and a bimodal (bi) scour distribution collected at an overbank event ($Q_p = 11.4$ m^3 s^{-1}) in the main channel. In each plot the straight line is Y = $\lambda + \alpha$X, where λ and α are the MLEs of the location and scale parameters of the fitted distributions, respectively.

shape parameters of one are equivalent to exponential distributions.

[21] The largest flow event in the Main Channel Reach exceeded bank-full and generated a right skewed bimodal scour depth distribution (Figure 4j). Although the RMSE associated with the exponential distributional fit is not particularly high (2.52 cm), it is clear that the model overestimates the frequency of shallow scour depths and underestimates the frequency of deep scour. The poorer fit of the exponential pdf to this scour depth distribution is clear from the significant nonlinearity shown by the probability plot (Figure 5d) and the relatively low PPCC (Table 4). The gamma and Weibull models perform somewhat better than the exponential model. Although a comparison of their respective probability plots (Figures 5l and 5p) and RMSE statistics (Table 4) suggests that the Weibull model performs slightly better than the gamma model, any distinction between the two pdfs in terms of model performance is of little significance as neither is an appropriate model for a bimodal distribution. With regard to the lognormal pdf, it is clear from the RMSE and PPCC

statistics (Table 4) and probability plots (Figures 5e–5h) that this model performs poorly at all but the lowest discharges.

[22] Distributions of fill depths for the nine within-bank flows are either monotonic and concave or right skewed (Figures 4k–4s). Monotonic distributions were obtained in six subbank-full events (Figures 4k–4m and 4o–4q). These distributions are described well by the gamma and Weibull models with RMSEs and PPCCs of 1.22–9.20 cm and 0.954–0.9966 respectively ($\overline{\text{RMSE}}$ = 4.04 cm; $\overline{\text{PPCC}}$ = 0.981) even though the probability plots reveal several outliers (e.g., Figures 6j and 6n). The shape parameters in all but two of the gamma and Weibull model fits are not significantly different from one (p < 0.05) indicating that the majority of the monotonic distributions are exponential in nature. A Weibull model conforming to the exponential pdf also fits one of the skewed distributions. The probability plots for the exponential model and the PPCC and RMSE statistics indicate that the monotonic distributions are equally well described by the simpler exponential model (Figures 7a and 7b and Table 4). The exponential model fits to the
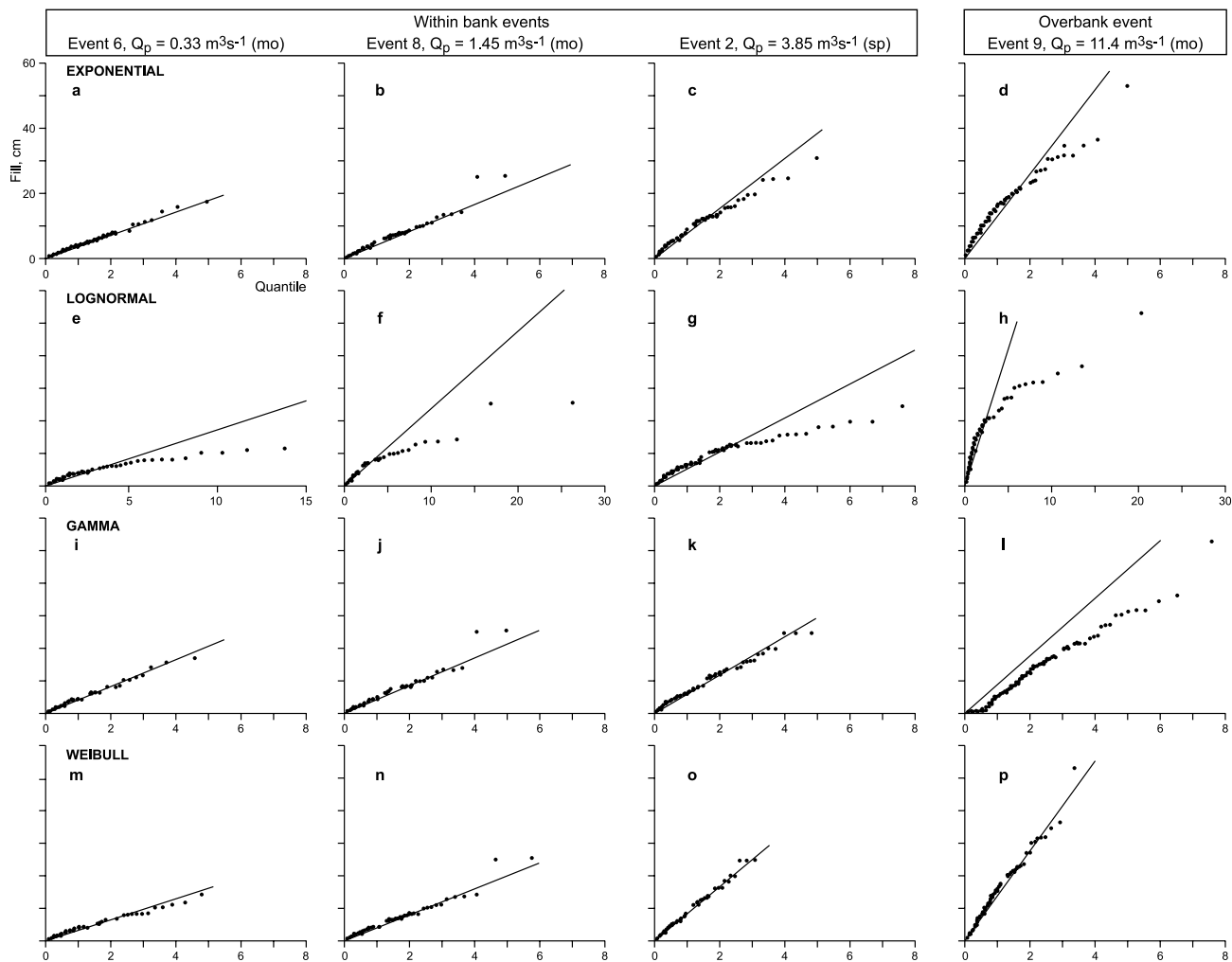
Figure 6. Probability plots for the theoretical pdfs fitted to monotonic (mo) and skew-peaked (sp) fill distributions obtained at discharges representative of low ($Q_p = 0.33$ m^3 s^{-1}), medium ($Q_p = 1.45$ m^3 s^{-1}), and high ($Q_p = 3.85$ m^3 s^{-1}) within-bank flow events and an overbank event ($Q_p = 11.4$ m^3 s^{-1}) in the main channel.

skew-peaked distributions generate PPCCs and RMSEs that are little different from those calculated for the monotonic distributions even though Figures 4n, 4r, and 4s clearly indicate that the exponential model overestimates the frequency of shallow fill depths and underestimates the frequency of deeper fill depths. The shortcomings of the exponential pdf for modeling skew-peaked events is, however, clearly revealed by the exponential probability plots which show that the left- and right-hand tails fall above and below the line representing $Y = \lambda + \alpha X$, respectively (e.g., Figure 6c). These systematic departures from linearity are not seen in the exponential probability plots for the monotonic distributions (see Figures 6a and 6b) and indicate that the observations in the tails of the skew-peaked distributions are closer to the distribution medians than they ought to be for samples drawn from an exponential distribution; i.e., the observed distributions have shorter tails [*Chambers et al.*, 1983, p. 206]. The probability plots indicate that the skew-peaked distributions are better described by the Weibull and gamma distributions (Figures 6k and 6o). Although the RMSEs and PPCCs suggest that the Weibull distribution performs somewhat better than the gamma distribution,

such a fine distinction in model performance may be unwarranted. As noted above, the discriminatory power of PPCCs and RMSE statistics appears to be limited by their insensitivity to small differences between the distributions under comparison.

[23] The distribution of fill depths associated with the overbank event is more irregular and platykurtic than those associated with within-channel events (Figure 4t). Comparison of the RMSE and PPCC statistics (Table 4) and probability plots for the four candidate models (Figure 6) indicate that the Weibull model provides the best distributional fit for this data set (RMSE = 2.07 cm; PPCC = 0.992). None of the fill distributions was described adequately by the lognormal pdf (Figures 4k–4t and 6e–6h).

[24] Representative frequency distributions of scour and fill depths for the upper and lower tributary reaches are shown in Figure 7. In both reaches, discharges were lower than in the main channel and depths of bed activity were consequently less. However, as in the main channel, higher flows generated greater depths of scour over an increasing proportion of the bed. At low discharges ($Q_p < $ c. 0.05 m^3 s^{-1}) bed activity in both reaches was limited to a few locations
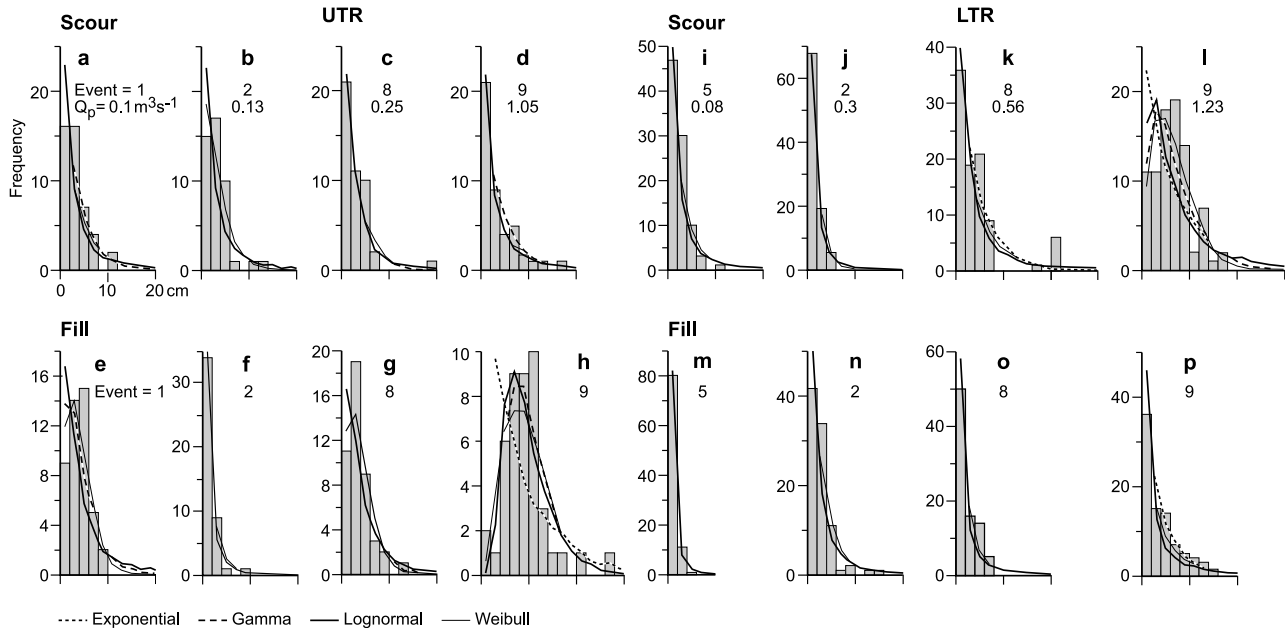
Figure 7. Frequency distributions of scour and fill for four representative events in the (a−h) upper and (i−p) lower tributary reaches.

and to generally less than 1−2 cm, whereas the highest flows ($Q_p \approx 1$ m^3 s^{-1}) generated more than 5 cm of scour over 75% of the bed area. Local maxima were 19 and 37 cm in the upper and lower tributaries, respectively. Depths of fill for individual events were comparable to depths of scour. For example, mean differences between paired depths of scour and fill in the lower tributary reach ranged from 0.7 ± 0.73 to 3.2 ± 2.5 cm with average differences of 1.2 ± 2.1 cm for the lowest five flows ($Q_p < 0.2$ m^3 s^{-1}) and 1.8 ± 2.1 cm for the four larger flows ($0.3 \leq Q_p \leq 1.2$ m^3 s^{-1}).

[25] As a result of limited bed activity (<2 cm), one of the fill distributions recorded in the upper tributary is restricted to one bin and cannot be subjected to analysis. The remaining 27 distributions exhibit similar shapes to those recorded in the main channel reach (compare Figures 4 and 7). All but two of the scour distributions recorded in the tributary reaches are monotonic and concave and are represented well by exponential, gamma and Weibull models ($\overline{\text{RMSE}}$ = 2.28, 2.42, 2.24 and $\overline{\text{PPCC}}$ = 0.942, 0.948 and 0.941 respectively). Half of the Weibull and gamma models fitted to the monotonic distributions conform to the exponential model (i.e., $\gamma = 1$; $p < 0.05$). Skew-peaked scour distributions were observed for events 2 and 9 in the upper and lower tributary reaches respectively. The former is characterized by Weibull and gamma models that are exponential in nature. The latter is fitted by Weibull and gamma distributions with $\gamma > 1$. Close comparisons of the observed and fitted frequency distributions and the associated probability plots indicate that the Weibull model yields slightly better descriptions of the skew-peaked distributions than are provided by either the gamma or exponential models (RMSE = 3.56, 4,26, 6.37 cm and PPCC = 0.930, 0.958, 0.973 respectively). Similar conclusions can be drawn about the fill distributions. The shapes of all but three are monotonic and concave; the monotonic distributions are described equally well by the exponential, gamma

and Weibull pdfs ($\overline{\text{RMSE}}$s = 2.68, 2.88, 2.79 cm and $\overline{\text{PPCC}}$s of 0.960, 0.967, 0.961 respectively); the majority (64%) of the gamma and Weibull models fitted to the monotonic distributions conform to the exponential model, whereas those fitted to the skew-peaked distributions do not; and the skew-peaked distributions (from events 1, 8 and 9 in the upper tributary reach) are best described by the Weibull pdf ($\overline{\text{RMSE}}$ = 2.57 cm, $\overline{\text{PPCC}}$= 0.966).

5.3. Model Evaluation

[26] Consideration of the RMSE and PPCC statistics together with the probability plots indicate that the lognormal distribution performs least well of the four theoretical distributions under consideration. It generates the highest RMSEs, the lowest PPCCs and the least satisfactory probability plots for both scour and fill distributions. Much better fits are provided by the exponential, gamma, and Weibull pdfs. In general, the observed distributions of scour and fill are equally well represented by these alternative models. However, more than half of the scour and fill distributions are modeled by Weibull and gamma pdfs with shape parameters of one rendering them equivalent to the exponential pdf. The monotonic and concave shape of the majority of the observed distributions suggests that the simpler exponential model may be adequate to model the reach−scale variability in scour and fill depths, particularly those that occur during within-channel flow events.

[27] To examine further the suitability of the exponential function, the similarity between the fitted and observed distributions was tested statistically using the Anderson-Darling test with a significance level of 0.95. The Anderson-Darling test is used in preference to the chi-square test because the minimum frequency requirement of the latter often resulted in insufficient degrees of freedom to conduct the test. The Anderson-Darling test indicates that 17 of the 28 scour distributions conform to the exponential model. All of the scour distributions successfully modeled by the
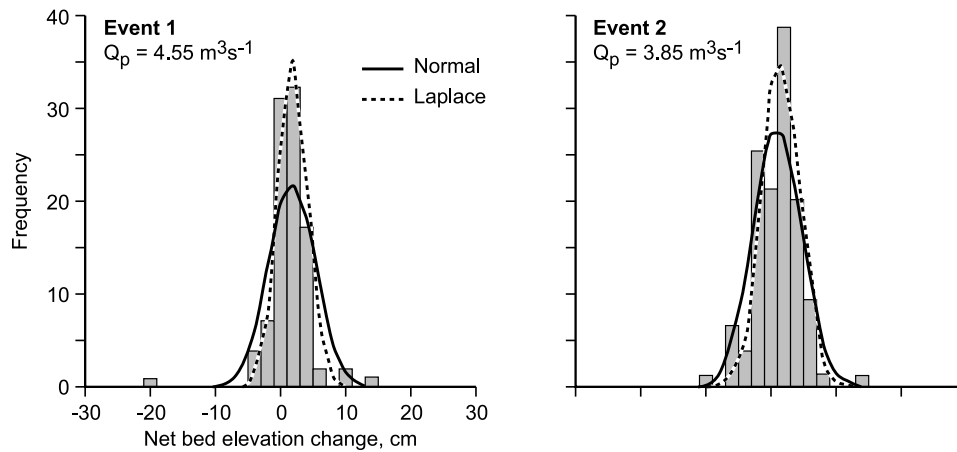
Figure 8. Frequency distributions of net change in streambed elevations for two events in the main channel reach.

exponential pdf are concave and monotonic. Of the 11 distributions that do not conform to the exponential model, eight are monotonic, two are skew-peaked and one is bimodal. Failure of the exponential pdf to model the skew-peaked and bimodal distributions is not surprising given the constraints on the shape of the exponential model (Table 3 and Figure 2). The failure of the exponential pdf to model the monotonic distributions occurs because it overestimates the frequency of low scour depths and underestimates the frequency of high scour depths. The exponential pdf is less successful at modeling the 27 fill distributions even though they have the same general shape as the scour distributions. Only nine fill distributions conform to the exponential model at a significance level of 0.05. The 18 nonconforming distributions comprise 12 monotonic and concave distributions and six skew-peaked distributions.

6. Discussion

[28] The analysis presented above addresses the first two questions posed in the introduction. Visual inspection of the fitted distributions and close inspection of PPCCs and RMSE statistics indicate that the gamma, Weibull, and exponential pdfs provide reasonable descriptive models for the reach-scale variability of scour and fill in the three study streams. Interestingly, however, many of the Weibull and gamma models conform to the exponential pdf (i.e., $\gamma \approx 1$). Nearly two thirds of the 28 scour distributions conform to the exponential model at a significance level of 0.95. The scale parameters show a correlation with discharge ranging from about 1.6 at low flows to about 14.7 at an overbank flow (Table 4). The correlation indicates that the distributions become stretched to the right as event discharge increases (see Figure 2a) and reflects the increasing depth of scour at progressively higher flows. Surprisingly, the location parameters approximate zero at all discharges indicating that despite highly mobile sand-sized sediment, scour did not occur across the channel bed at discharges up to and in excess of the bank-full discharge. This observation is contrary to the expectation that the whole bed would be scoured at quite modest discharges

and that minimum depths of bed lowering during an event would increase significantly with discharge (e.g., Figure 3).

[29] In contrast, although the majority of fill distributions exhibit monotonic and concave shapes, the Anderson Darling test demonstrates a general disparity between the exponential models and the measured distributions with the null hypothesis (that the data conform to the models) being rejected in 67% of the cases. That scour distributions are adequately fitted by an exponential model, whereas fill distributions are not raises interesting questions about the notion of quasi-equilibrium channel form and the role of scour and fill in effecting channel change. Detailed analyses of the spatial patterns of scour and fill and their relationship to longer-term measurements of channel change based on cross-section surveys [*Nichols*, 1999] are being undertaken to shed some light on this role. Interestingly, distributions of event-based estimates of net changes in streambed elevations (i.e., − scour depths + fill depths) show similarities to the Laplace distribution (Figure 8). The Laplace distribution has a similar shape to the normal distribution but is more leptokurtic. It is defined as distribution of differences between two independent variates with identical exponential distributions [*Abramowitz and Stegun*, 1972, p. 930].

[30] Even for scour, there is some suggestion that there is a change in the shape of the distribution for larger flow events (and, particularly, overbank events). However, the significance of these distributions cannot be assessed with the present data set because they are too few in number, and further data obtained at high flows are required to resolve whether increases in flow strength generate systematic changes in the shape of scour and fill distributions as hypothesized in Figure 3 and suggested by *Hassan et al.* [1999].

[31] For scour, the inverse relation between the exponential model parameters and peak flow can be used to produce a model for predicting depths of scour (question three) similar to that shown by *Haschenburger* [1999] for gravel bed streams. Figure 9 shows that exponential model parameters collapse onto a general trend when rated against the bed shear stress in excess of a threshold value (τ_c). A value for τ_c was estimated from the scour chain record. As noted above, three events in the lower tributary reach exerted
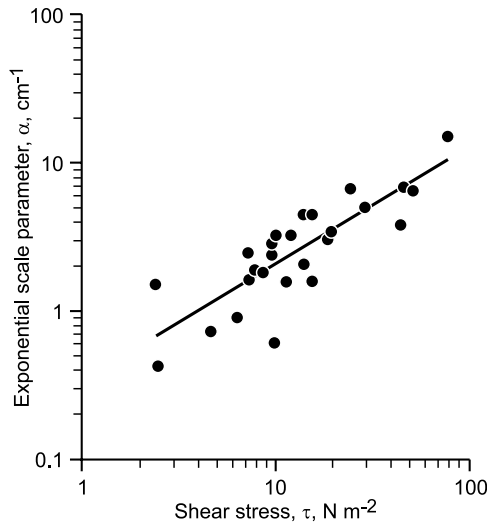
Figure 9. Relation between exponential model parameter and excess shear stress.

Notation

α scale parameter.
γ shape parameter.
Γ gamma function.
λ location parameter.
ρ density of flow, $kg\ m^{-3}$.
τ shear stress, $N\ m^{-2}$.
τ_c critical shear stress, $N\ m^{-2}$.
D_{50} median particle size, mm.
g acceleration due to gravity, $m\ s^{-2}$.
n number of bin classes.
Q_p peak discharge, $m^3\ s^{-1}$.
R hydraulic radius, m.
S bed slope, $m\ m^{-1}$.
x_o observed frequencies of depths falling with specified bin classes.
x_p predicted frequencies of depths falling with specified bin classes.

maximum shear stresses of between 6 and 8.5 N m^{-2} (peak water depths of approximately 0.05 and 0.07 m, respectively). On these occasions, the scour chains registered only limited and patchy movement of bed material suggesting conditions approaching incipient motion. If, in the light of this, a water depth of 0.05 m is taken as critical and the local bed slope of 0.0173 is used, then $\tau_c = 6.1$ N m^{-2}. The resultant least squares relation is

$$\alpha = 0.34(\tau - \tau_c)^{0.78}.$$

It explains 68% of the variance ($p < 0.05$) and provides a means to estimate the distribution of scour depths to a first approximation in similar streams when only flow and sediment characteristics are known.

7. Conclusions

[32] In this study we have undertaken a detailed analysis of scour and fill during 10 flood events along three reaches of low-order sand bed, dryland rivers. The density of measurements obtained from this study exceeds that of previous studies by two to three orders of magnitude. Our analysis of the distributions of scour and fill depths reveals that of four distribution functions fitted (lognormal, exponential, gamma, and Weibull) all but the first of them successfully models the distributions of scour depths. Inasmuch as the exponential distribution is the simplest of the three successful fits, it is proposed here as an adequate model to describe the distribution of scour depths in sand bed channels over the range of flows studied. The inverse relation between the parameters of this distribution and peak excess shear stress defines a general relationship that can be used to estimate the magnitude of scour in sand bed streams, at least to a first approximation. The disparity between the distributions of scour and fill raises questions about the role of scour and fill in effecting channel change. These questions will be addressed in a subsequent paper through a detailed examination of the spatial patterns of scour and fill within reaches.

References

Abramowitz, M., and I. A. Stegun (1972), *Handbook of Mathematical Functions With Formulas, Graphs, and Mathematical Tables*, Dover, Mineola, N. Y.

Andrews, E. D. (1979), Scour and fill in a stream channel, East Fork River, Wyoming, *U.S. Geol. Surv. Prof. Pap., 1117*.

Chambers, J. M., W. S. Cleveland, B. Kleiner, and P. A. Tukey (1983), *Graphical Methods for Data Analysis*, Wadsworth, Belmont, Calif.

Chang, H. H. (1988), *Fluvial Processes in River Engineering*, John Wiley, Hoboken, N. J.

De Vries, P., S. J. Burges, J. Daigeau, and D. Stearns (2001), Measurement of the temporal progression of scour in a pool-riffle sequence in a gravel-bed stream using an electronic scour monitor, *Water Resour. Res., 37*, 2805–2816.

Emmett, W. W., and L. B. Leopold (1965), Downstream pattern of river-bed scour and fill, in *Federal Inter-agency Sedimentation Conference Proceedings, Jackson, Miss.*, pp. 399–409, U.S. Gov. Print. Off., Washington, D. C.

Foley, M. G. (1971), Scour and fill in steep, sand-bed ephemeral streams, *Geol. Soc. Am. Bull., 89*, 559–570.

Haschenburger, J. (1999), A probability model of scour and fill depths in gravel-bed channels, *Water Resour. Res., 35*, 2857–2869.

Hassan, M. A., M. Church, and A. P. Schick (1991), Distance of movement of coarse particles in gravel bed streams, *Water Resour. Res., 27*, 503–511.

Hassan, M. A., A. P. Schick, and P. A. Shaw (1999), The transport of gravel in an ephemeral sandbed river, *Earth Surf. Processes Landforms, 24*, 623–640.

Filliben, J. J. (1975), The probability plot correlation coefficient test for normality, *Technometrics, 17*, 111–117.

Johnson, N. L., S. Kotz, and N. Balakrishnan (1994), *Continuous Univariate Distributions*, vol. 1, 2nd ed., John Wiley, Hoboken, N. J.

Kondolf, G. M., and A. Adhikari (2000), Weibull vs lognormal distributions for fluvial gravels, *J. Sediment. Res., 70*, 456–460.

Lane, E. W., and W. M. Borland (1954), River-bed scour during floods, *Trans. Am. Soc. Civil Eng., 119*, 1069–1089.

Lane, L. J., M. Hernandez, and M. Nichols (1997), Processes controlling sediment yield from watersheds as a function of spatial scale, *Environ. Modell. Software, 12*, 335–369.

Lapointe, M., B. Eaton, S. Driscoll, and C. Latulippe (2000), Modelling the probability of salmonid egg pocket scour due to floods, *Can. J. Fish. Aquat. Sci., 57*, 1120–1130.

Laronne, J. B., D. N. Outhet, P. A. Carling, and T. J. McCabe (1994), Scour chain deployment in gravel-bed rivers, *Catena, 22*, 299–306.

Leopold, L. B., and T. Maddock (1953), The hydraulic geometry of stream channels and some physiographic implications, *U.S. Geol. Surv. Prof. Pap.*, *252*.

Leopold, L. B., W. W. Emmett, and R. M. Myrick (1966), Channel and hillslope processes in a semi-arid area, New Mexico, *U.S. Geol. Surv. Prof. Pap.*, *352G*.

Nichols, M. N. (1999), The spatial distribution of sediment sources and sinks at the watershed scale in semi-arid areas, Ph.D. thesis, N. M. State Univ., Las Cruces.

Paola, C., and L. Borgman (1991), Reconstructing random topography from preserved stratification, *Sedimentology*, *38*, 553–565.

Renard, K., and R. V. Keppel (1966), Hydrographs of ephemeral streams in the southwest, *Proc. Hydraul. Div. Am. Soc. Civ. Eng.*, *92*, 33–52.

Renard, K., and E. M. Laursen (1975), Dynamic behaviour model of ephemeral stream, *Proc. Hydraul. Div. Am. Soc. Civ. Eng.*, *101*, 511–528.

Rennie, C. D., and R. G. Millar (2000), Spatial variability of stream bed scour and fill: A comparison of scour depth in chum salmon (*Oncorhynchus keta*) redds and adjacent bed, *Can. J. Fish. Aquat. Sci.*, *57*, 928–938.

Takle, E. S., and J. M. Brown (1978), Note on the use of Weibull statistics to characterize wind speed data, *J. Appl. Meteorol.*, *17*, 556–559.

The MathWorks (2000), MATLAB: The Language of Technical Computing, software, Natick, Mass.

Zobeck, T. M., T. E. Gill, and T. M. Popham (1999), A two-parameter Weibull function to describe airborne dust particle size distributions, *Earth Surf. Processes Landforms*, *24*, 943–955.

————————————

R. Brazier and J. Wainwright, Department of Geography, University of Sheffield, Sheffield, S10 2TN, UK.

J. Kaduk, A. Parsons, and D. M. Powell, Department of Geography, University of Leicester, Leicester, LE1 7RH, UK. (dmp6@le.ac.uk)